IOP Publishing Journal of Physics: Condensed Matter

J. Phys.: Condens. Matter **22** (2010) 305004 (6pp) doi:10.1088/0953-8984/22/30/305004

Secondary electron emission spectra from clean and cesiated Al surfaces: the role of plasmon decay and data analysis for applications

P Riccardi[1,3], M Pisarra[1], A Cupolillo[1], M Commisso[1], A Sindona[1], R A Baragiola[2] and C A Dukes[2]

[1] Dipartimento di Fisica, Università della Calabria and INFN gruppo Collegato di Cosenza, I-87036 Rende, Cosenza, Italy

[2] Engineering Physics, University of Virginia, Charlottesville, VA 22904, USA

E-mail: riccardi@fis.unical.it

Received 22 March 2010, in final form 24 May 2010
Published 7 July 2010
Online at stacks.iop.org/JPhysCM/22/305004

Abstract

We report measurements of energy spectra of secondary electrons emitted from clean and cesiated aluminum surfaces under the impact of 130 eV electrons. Measurements show that the decay of bulk and surface plasmons dominates the electron emission. In contrast with theoretical calculations, our experiments indicate that the electron collision cascade inside the solid produced by electrons excited by plasmon decay do not contribute significantly to electron emission.

A simple analysis of electron energy distributions measured as a function of Cs surface coverage allows separation of rediffused incident electrons from the continuum background of true secondary electrons. The result shows that yields of rediffused electrons used in several applications may have been significantly overestimated.

(Some figures in this article are in colour only in the electronic version)

1. Introduction

Secondary electrons (SE) are those electrons of a target material that are emitted in vacuum by the impact of energetic (primary) particles. The phenomenon is the basis for several spectroscopic techniques for surface analysis and characterization of materials [1, 2], as well as for the scanning electron microscope [3]. Secondary electron emission also plays a crucial role in a wide variety of areas, including electron multipliers, electrical discharge and plasma processing of materials [4], particle accelerators and plasma–wall interactions in fusion reactors [5]. Electron emission may be a problem that needs to be avoided or reduced, such as electron cloud effects in high energy accelerators and storage rings [6]. Progress in all these areas call for advances in the basic understanding of electron emission in particle–solid interactions. This motivates the study of the energy distribution of emitted electrons $N(E)$ and of its integral, the electron emission yield δ, as a function of several variables, such as impact energy, incidence and emission angles, as well as surface conditions.

Electrons excited by the projectile inside the solid undergo multiple collisions with other electrons in the solid (inelastic scattering) and with the ionic cores (elastic scattering). Electron emission occurs when this collision cascade is interrupted by the surface and the excited electrons have energies above the vacuum level. When the primary particles are electrons, the part of $N(E)$ due to secondary electrons overlaps with that of primary electrons that have been reflected from the solid [7, 8]. In this case, $N(E)$ contains a sharp peak due to primary electrons elastically reflected (*elastic peak*) and nearby structure on the low energy side due to energy losses of reflected primary electrons (also termed *rediffused*). Sharp peaks in that structure contain electrons that lost energy

[3] Author to whom any correspondence should be addressed.

in excitation of a discrete number of surface and volume plasmons [9]. Evidence of plasmon excitation also appears in the low energy part of $N(E)$ of some solids [10–13] as a structure containing electrons across the valence band that can be excited by plasmon decay above the vacuum level [13]. The plasmon decay structure is often difficult to visualize because it is superimposed on the low energy part of the collision cascade. This factor hinders the, yet unanswered, question of the quantitative contribution of plasmon decay to the total secondary electron emission

The energies of electrons excited by the decay of plasmons of energy $E_{\rm pl}$ with respect to the vacuum level range from a maximum $E_{\rm m} = E_{\rm pl} - \Phi$ to a minimum $E_{\rm m} - W$, corresponding to the absorption of the plasmon energy by an electron at the Fermi level and one from the bottom of the valence band, respectively. Here, W is the width of the valence band and Φ is the work function of the surface. Though discussed for decades [10], the plasmon decay lineshape in aluminum surfaces has been directly revealed only very recently by measurements of the SE spectrum in coincidence with features due to the excitation of surface and bulk plasmons in the energy loss spectrum of reflected primary electrons [13]. Coincidence measurements, however, do not reveal the decay of those plasmons that are excited indirectly by secondary electrons and, therefore, cannot address the contribution of plasmon decay electrons to the total electron emission yield.

As mentioned above, visualization of the plasmon decay structures in $N(E)$ is often difficult; it is usually enhanced by taking the derivative $\mathrm{d}N/\mathrm{d}E$ [10, 12], which shows a minimum at the maximum energy, $E_{\rm m}$. Theoretical calculations [10, 11] show that the inclusion of surface and bulk plasmon decays is essential to reproduce the spectra (and the derivatives) of electrons emitted from aluminum surfaces under energetic electron bombardment. Furthermore, the agreement with experimental data is significantly improved by the inclusion of electrons produced in the collision cascade initiated by plasmon decay electrons inside the solid.

In this work, we investigate the role of plasmon decay in secondary electron emission through measurements of energy spectra of electrons emitted by 130 eV and 2 keV electron impact on clean and cesiated Al surfaces [14]. The measurements demonstrate the dominance of plasmon decay in secondary electron emission at impacting electron energies close to the threshold for plasmon excitation. In contrast with theoretical calculations [10, 11], our experiments indicate that cascade electrons excited by plasmon decay do not contribute significantly to electron emission.

The data allow us also to discuss an issue that is important in many phenomena and applications, where electron emission is a relevant process. Many of these phenomena are studied by means of simulation codes [4, 6] that show a strong sensitivity to parameters pertaining to the electron emission yield δ and the energy distribution of emitted electrons $N(E)$. The reliability of electron yields extracted from experimental energy spectra is therefore an important requirement. Our data allow us to illustrate a very simple data analysis procedure to accomplish this requirement, particularly for those applications where electron reflection is important.

2. Experiments

The experiments were done in ultrahigh vacuum ($\sim 1 \times 10^{-10}$ Torr) in a Physical Electronics 560 x-ray photoelectron spectroscopy (XPS) and Auger microprobe system equipped with a double-pass cylindrical mirror electron energy spectrometer used previously for other studies of ion- and electron-induced electron emission from surfaces [12]. To measure accurately low energy electrons the chamber was shielded with μ-metal to reduce the effect of stray magnetic fields. For these experiments, the spectrometer was operated at constant pass energy, $E = 40$ eV, with an energy resolution of 0.2 eV.

The electron beam from a thermionic source was collinear to the axis of the spectrometer and impinged on the sample at an angle of 30° with respect to the surface normal. The high-purity polycrystalline surfaces were sputter-cleaned by 4 keV Ar ions. The sputtering was continued beyond that required to remove any detectable level of contamination by Auger spectroscopy until the structure in the electron energy spectra remained constant.

Cs atoms were deposited on the Al surface at 20 °C using dispensers from SAES getters at a constant rate. Each deposition step was followed by the measurement of $N(E)$. The most evident effect of Cs deposition is the downward shift in the low energy cutoff in $N(E)$ due to the lowering of the work function [14]. Absolute calibration of the coverage may be derived from the variation of the intensity of Cs and Al Auger lines, but this is not essential for the purpose of this paper.

3. Results

Figures 1–3 report the electron energy spectra revealed in our experiments due to the impact of electrons with energy $E_0 = 130$ eV on the clean and cesiated Al surface. The experiments have been conducted with the sample biased at a negative potential with respect to ground $V_{\rm b} = -5$ V to observe the emission threshold at the vacuum level of the sample. All the spectra in figures 1–3 have been acquired with a constant beam current and have been corrected for the energy-dependent optical transmission of the analyzer [15] we measured for our instrument.

Figure 1 shows the spectrum of electrons ejected from a clean Al sample. The electrons giving rise to the spectrum of figure 1 can be divided into three main groups [15–20]: (i) elastically reflected electrons (EE), (ii) rediffused electrons (RE) and (iii) true secondary electrons (SE). EEs are primary electrons of the beam that have been reflected without suffering energy loss in the interaction with the target material, resulting in the *elastic peak* at $E = E_0$. Rediffused electrons are reflected primary electrons that have suffered inelastic energy losses. An energy loss $E_{\rm L}$ will give rise to a structure at an energy $E = E_0 - E_{\rm L}$. In the case of Al samples the spectrum of the rediffused electrons is dominated by the structures due to primary electrons that have suffered multiple energy losses in excitation of surface and bulk plasmons of the sample ($E_{\rm p} = 15.3$ eV and $E_{\rm s} = 10.8$ eV are, respectively, the energies

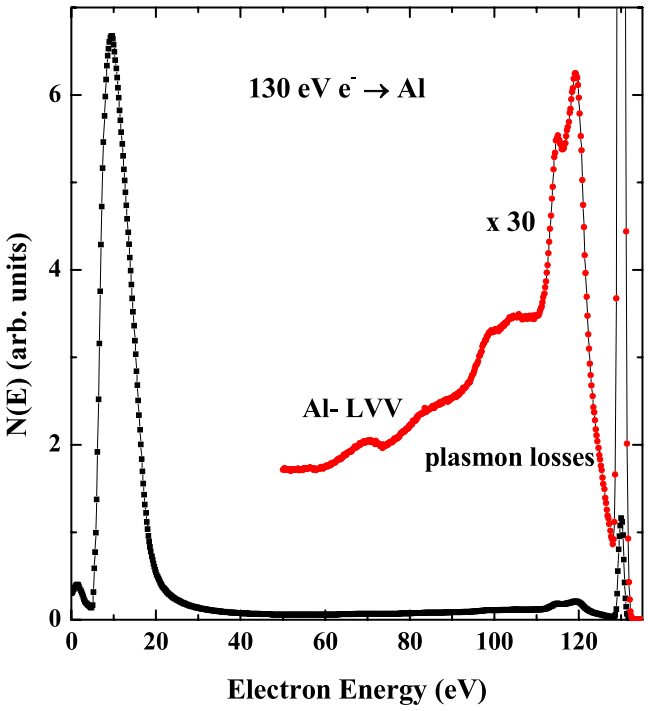

Figure 1. Energy spectrum of electron emitted from a sputter-cleaned Al sample due to the impact of electrons with energy $E_0 = 130$ eV. The portion of the spectrum between 50 eV and the onset of the elastic peak is amplified to show the plasmon losses and the Al-LVV Auger emission.

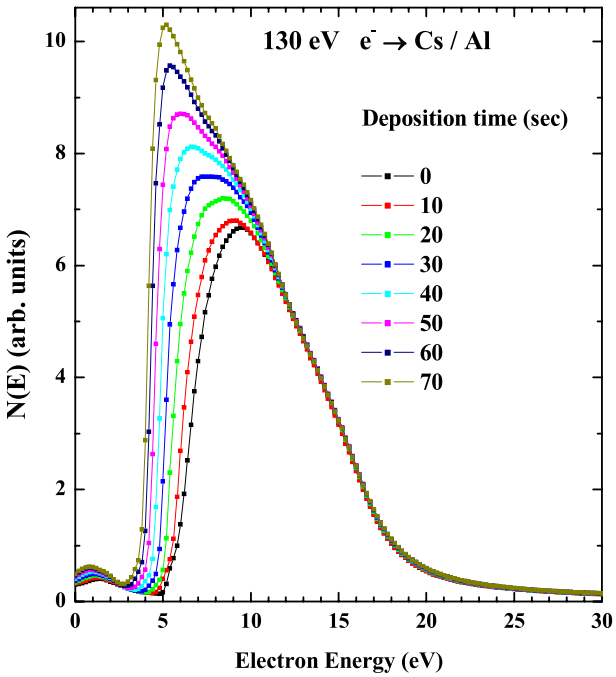

Figure 2. Low energy region of the electron emission spectra acquired after sequential deposition of Cs atoms. The spectra have been acquired at constant beam current and corrected for the analyzer transmission. Cs deposition is expressed in terms of the total deposition time. The shift towards low energies of the emission threshold reflects the reduction of the metal work function Φ due to Cs deposition [14].

of the low momentum bulk and surface plasmon in Al). All the other emitted electrons are counted into the spectrum of true secondary electrons that contains the vast majority of emitted electrons, including the Al-LVV Auger electrons. This spectrum is characterized by a broad distribution, showing a peak at low electron energy. The high energy tail of the true secondary electron spectrum produces a smooth background below the energy loss electron structure.

Figure 2 shows the low energy region of the electron emission spectra, measured at constant beam current and acquired after sequential deposition of Cs atoms. The shift towards low energies of the emission threshold reflects the reduction of the metal work function Φ due to Cs deposition [14].

Figure 3 shows the pronounced effect of Cs deposition on the spectrum of rediffused and elastically reflected electrons.

4. Discussion

4.1. The role of plasmon decay

Figure 4 shows the comparison of the low energy region of the spectrum in figure 1 with a spectrum induced by 2 keV electrons. Both spectra have been acquired with the sample biased at a negative voltage with respect to ground $V_b = -5$ V. Also shown in figure 4 is the spectrum acquired at 2 keV impact energy without bias voltage, which shows that the bias does not produce significant changes in the shape of the spectra. To compare shapes, all the spectra in figure 4 have been normalized so that their areas are equal.

The spectrum due to 2 keV electron impact is consistent with spectra found in the extensive literature published on the topic [10–12] and is dominated by the peak at low electron energy. This feature includes contributions from directly excited secondary electrons, as well as from the inelastic collision cascade of secondary electrons. Theoretical calculations [10, 11] suggested that electrons produced in the cascade initiated by plasmon decay electrons inside the solid might give an important contribution to this spectral feature. For keV electrons, the tail of the low energy peak forms a continuous background that is superimposed with discrete structures due to electron emission from the decay of low momentum q surface and bulk plasmons [10, 12]. These structures are more clearly visualized in the derivative $dN(E)/dE$ [10, 12]. This is also shown in figure 3, where the plasmon features result in the minima observed in the derivative at energies $E_m = E_{pl} - \Phi + |V_b|$, $(6.5 + |V_b|)$ eV and $(11 + |V_b|)$ eV, corresponding to surface and bulk plasmons with momentum $q = 0$, respectively ($\Phi = 4.3$ eV for polycrystalline Al). At 130 eV impact energy, the low energy (cascade) peak is strongly reduced and the spectrum appears to be dominated by the plasmon decay features, primarily the bulk plasmon with its clear edge. The distinct increase in the importance of the plasmon decay electrons in the low energy spectra seen in figure 3 indicates that the collision cascade initiated by electrons excited by plasmon decay and scattered inside the solids is not as important as previously assumed [10, 11].

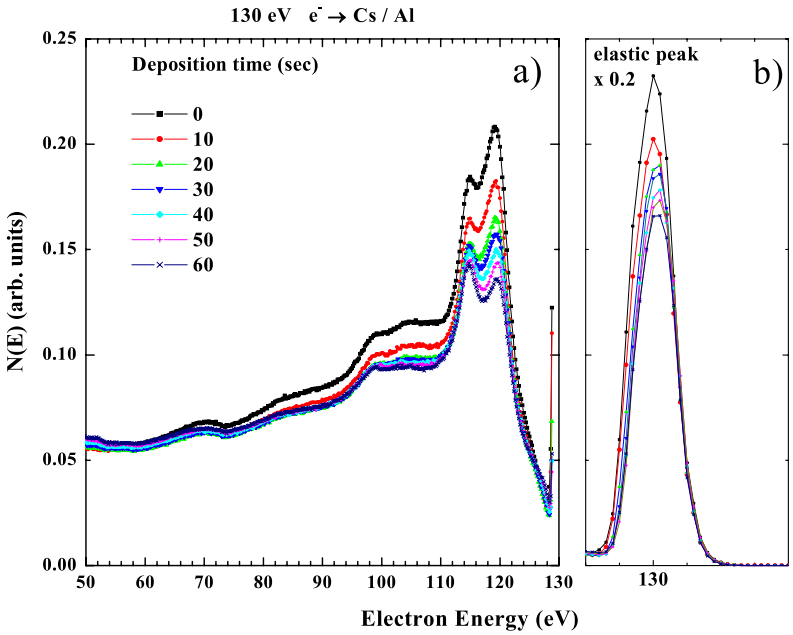

Figure 3. Region of the spectra of rediffused (a) and elastic (b) electrons acquired after sequential deposition of Cs atoms. The spectra have been acquired at constant beam current and corrected for the analyzer transmission. The width of the elastic peak is mainly determined by the thermal energy spread of the thermionic electron source.

The measurements performed after modification of the surface by depositing Cs atoms (figures 2 and 3) show the increase of the emission yield upon Cs adsorption due to the decrease of the work function. We observe in figure 2 that Cs deposition alters the spectrum of true secondary electrons at very low energies, revealing electron excitations at energies below the original vacuum level which is lowered by Cs deposition. Figure 2 show also that Cs deposition does not affect significantly the high energy tail of the spectrum of the true secondary electrons, including the bulk plasmon decay feature that is still characterized by its clear edge, as also shown in figure 5 containing the derivatives of the spectra in figure 2. These observations suggest an important role of energetic electrons from the collision cascade in determining bulk plasmon excitation, similar to the case of kinetic ion-induced electron emission [21]. On the other hand, in figure 3 we observe a noticeable variation of the components of the spectrum due to electron reflection (either elastic and inelastic), with the bulk features obviously less affected than the surface ones.

Figure 5 shows an apparent increase of the surface plasmon dip in the derivative. This can be explained by the concurrent presence of growing low energy structures due to the Auger decay of Cs atoms excited in the $5p_{1/2}$ and $5p_{3/2}$ states [22].

4.2. Analysis of electron emission spectra for practical purposes

The data allow us to discuss an issue that is important for applications that require secondary electron emission yields, particularly those where electron reflection is important. Recently, the role of reflected electrons has been experimentally investigated in the case of cesiated Cu samples used in plasma sources of negative hydrogenic ions [23, 24] and in the case of materials used in particle accelerators [6, 16]. In this last case, the results of simulations of the generation of an electron cloud in the beamline were significantly affected by the inclusion of elastic and rediffused electrons, compared to the case where only secondary electrons were taken into account [6, 16]. As they may constitute input to simulation codes that base their validity on the reliability of these data, it is clear that electron emission yields have to be extracted from experimental energy spectra as accurately as possible.

The yield δ_s of true secondary electrons is usually extracted from the measured electron spectrum integrating the spectrum up to 50 eV [16, 18, 19]. The area of the spectrum between 50 eV and the onset of the elastic peak gives δ_r, the yield of rediffused electrons. The total emission intensity is therefore given by $\delta = \delta_e + \delta_r + \delta_s$, where δ_e is the area of the elastic peak.

Our data are an example of the fact that the spectrum of secondary electrons may extend up to energies well above 50 eV, as is made clear by the LVV-Al Auger structure and background below the energy loss peaks. However, this energy is widely considered a good threshold to distinguish the two types of electrons leaving the sample, since the yield of secondary electrons with more than 50 eV energy is small compared to δ_s. In many cases, however, this contribution may need to be subtracted from δ_r to obtain a reliable estimate of the yield of rediffused electrons. A simple procedure to separate these two components is shown in figure 6, where the continuous background spectrum of secondary electrons is modeled by fitting two energy regions, before and after the rediffused and elastic energy range, with a smoothly decreasing polynomial function. A polynomial function was utilized for simplicity; other frequently used functional forms [25, 26] give very similar results. The background spectrum is then

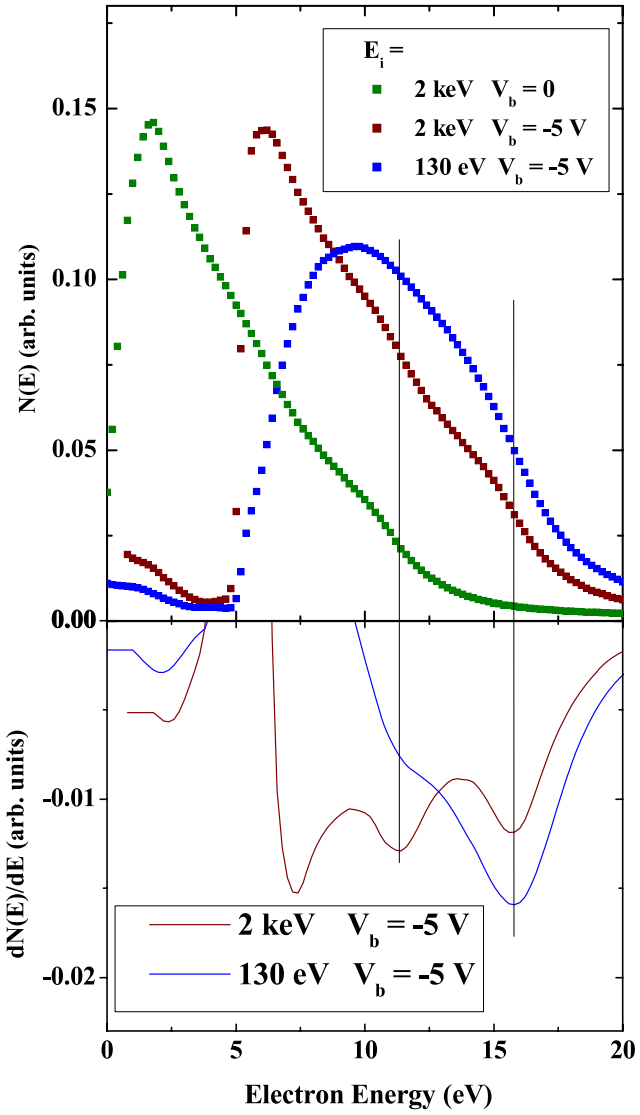

Figure 4. Top: energy spectra of electrons emitted by the Al surface bombarded by 130 eV and 2 keV electrons acquired with the sample biased at a negative voltage $V_b = -5$ V. The spectrum acquired under bombardment with 2 keV electrons without biasing the sample is also reported for comparison. All the spectra have been normalized so that their areas equal unity. Bottom: derivative of $dN(E)/dE$ that enhances the structure due to plasmon decay. The vertical lines mark the plasmon edges.

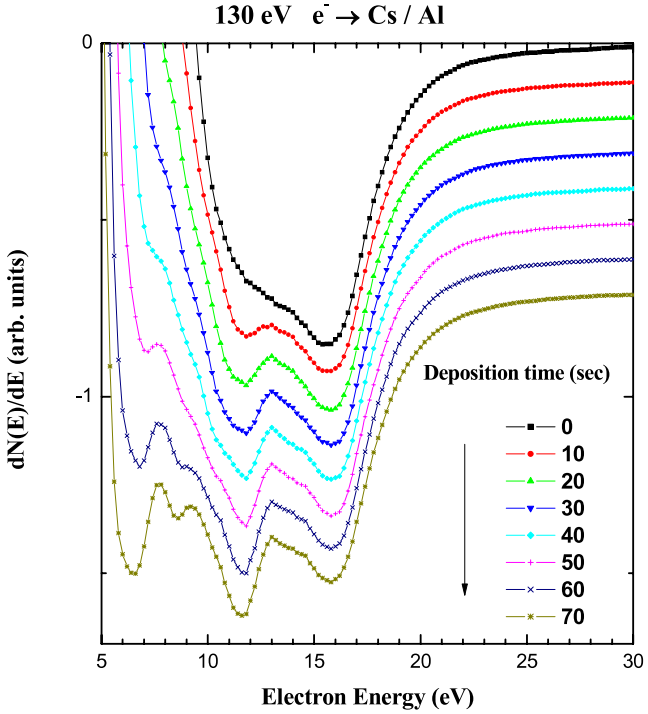

Figure 5. Derivatives of the spectra reported in figure 2. The curves are shown arbitrarily displaced on the vertical scale for clarity.

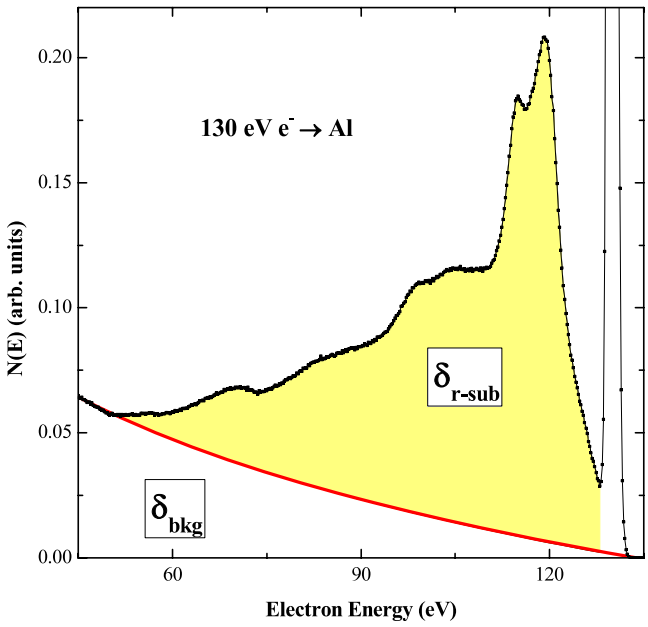

Figure 6. Example of subtraction of the background spectrum to obtain the yield δ_{r-sub} (dashed area) of rediffused electrons.

subtracted from the measured spectrum to yield the 'true' rediffused spectrum, whose area gives the new value δ_{r-sub}. For the sake of simplicity, we did not consider Auger electrons in our analysis as their contribution is very small and can be easily subtracted, if needed. The uncertainty in the values of $\delta_{r,sub}$ is estimated to be about 15% by varying the function that represents the background and the energy regions where the fitting procedure is applied.

In our case $\delta_{r,sub}$ is significantly smaller than δ_r. Furthermore, we observe that $\delta_{r,sub}$ shows the same dependence on Cs coverage as the area of the elastic peak δ_e, as shown in figure 7 by the constancy of the ratio $R_{sub} = \delta_{r,sub}/\delta_e$. In contrast, we observe that this is not the case for the ratio $R = \delta_r/\delta_e$, which increases with Cs deposition, further stressing the need of data analysis to disentangle contributions to the total electron yields.

5. Conclusions

Measurements of electron bombardment of clean and cesiated Al surfaces at 130 eV give insight into the role of plasmon

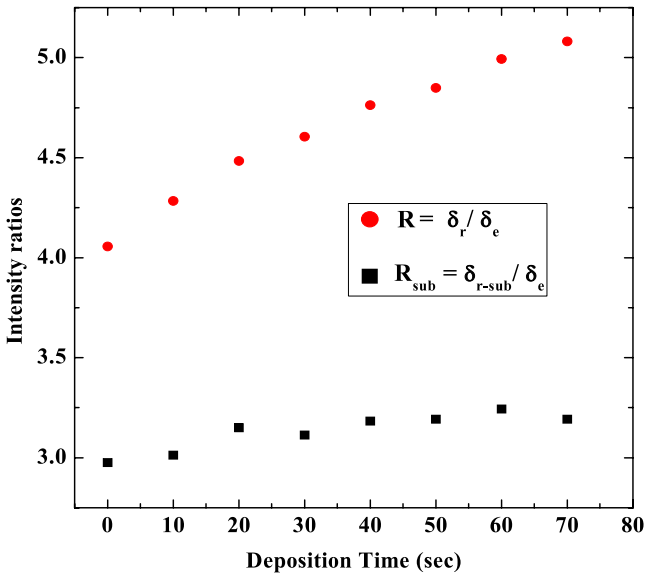

Figure 7. Intensity ratios $R_{\mathrm{sub}} = \delta_{\mathrm{r,sub}}/\delta_{\mathrm{e}}$ and $\mathrm{R} = \delta_{\mathrm{r}}/\delta_{\mathrm{e}}$ as a function of Cs deposition time.

decay in secondary electron emission. Electron emission from a clean metal surface appears to be dominated by plasmon decay features. The electron collision cascade excited by plasmon decay appears not to be as important as considered in theoretical calculations.

The data show that the choice of an upper energy cutoff at 50 eV for the spectrum of true secondary electrons may lead to values of yields of rediffused electrons being significantly overestimated. More generally, the interplay between different emission mechanisms in many cases cannot be neglected, as electrons of different origins can have the same characteristic energy. This implies that application of data analysis techniques to experimental spectra is required whenever there is the need to disentangle different contributions to the electron emission yield [27]. Whereas theoretical analysis of spectra of rediffused electrons is nowadays available [8], in many cases knowledge of the details of the electron energy distribution is not needed. Our simplified analysis provides a prompt tool to decide whether the yield of rediffused electrons is correctly estimated and to separate the spectrum of rediffused electrons from the continuum background of cascade electrons. Furthermore, the separation may be important because the behavior of the two components of the spectrum above 50 eV might change with surface conditions, as in the experiments reported here, as well as with impact energy, incidence and emission angles. Indeed this has been recently observed in angular measurements of energy distributions of secondary electrons emitted from samples of the Cu surface used in the Large Hadron Collider (LHC) Beam Screen [28].

References

[1] Briggs D and Seah M P 1990 *Practical Surface Analysis: Auger and X-Ray Photoelectron Spectroscopy* (Chichester, NY: Wiley–Interscience)

[2] Hagstrum H D 1971 *Phys. Rev.* **4** 4187

[3] Reimer L 1985 *Scanning Electron Microscopy* (Berlin: Springer)

[4] Baragiola R A and Riccardi P 2008 *Reactive Sputter Deposition* (*Springer Series in Material Science* vol 109) ed D Depla and S Mahieu, chapter 2

[5] Fubiani G, de Esch H P L, Simonin A and Hemsworth R S 2008 *Phys. Rev. ST Accel. Beams* **11** 014202

[6] Cimino R, Collins I R, Furman M A, Pivi M, Ruggiero F, Rumolo G and Zimmermann F 2004 *Phys. Rev. Lett.* **93** 014801

[7] den Boer M L, Cohen P I and Park R L 1978 *J. Vac. Sci. Technol.* **15** 502

[8] Werner W S M, Glantsching K and Ambrosch-Draxl C 2009 *J. Chem. Phys. Ref. Data* **38** 1013
Werner W S M 2006 *Phys. Rev.* B **74** 075421

[9] Raether H 1980 *Excitation of Plasmons and Interband Transitions by Electrons* (*Springer Tracts in Modern Physics* vol 88) (Berlin: Springer)

[10] Chung M S and Everhart T E 1977 *Phys. Rev.* B **15** 4699

[11] Rösler M and Brauer W 1988 *Phys. Status Solidi* **148** 213

[12] Baragiola R A and Dukes C A 1996 *Phys. Rev. Lett.* **76** 2457

[13] Werner W S M, Ruocco A, Offi F, Iacobucci S, Smekal W, Winter H P and Stefani G 2008 *Phys. Rev.* B **78** 233403

[14] Bonzel H P, Bradshaw A M and Ertl G (ed) 1989 *Physics and Chemistry of Alkali Metal Adsorption* (*Mat. Sci. Monographs no. 57*) (Amsterdam: Elsevier)

[15] Powell J C and Seah M P 1990 *J. Vac. Sci. Technol.* A **8** 735

[16] Furman M A and Pivi M T F 2002 *Phys. Rev. ST Accel. Beams* **5** 124404
Furman M A and Chaplin V H 2006 *Phys. Rev. ST Accel. Beams* **9** 034403

[17] Werner W S M 2007 *Slow Heavy-Particle Induced Electron Emission from Solid Surfaces* (*Springer Tracts in Modern Physics* vol 225) ed H P Winter and J Burgdorfer, chapter 2

[18] Walker C G H, El-Gomati M M, Assa'd A M D and Zadražil M 2008 *Scanning* **30** 365–80

[19] Lin Y and Joy D C 2005 *Surf. Interface Anal.* **37** 895

[20] Seiler H 1983 *J. Appl. Phys.* **54** R1

[21] Ritzau S M, Baragiola R A and Montreal R C 1999 *Phys. Rev.* B **59** 15506
Commisso M, Minniti M, Sindona A, Bonanno A, Oliva A, Baragiola R A and Riccardi P 2005 *Phys. Rev.* B **72** 165419
Cupolillo A, Pisarra M, Sindona A, Commisso M and Riccardi P 2010 *Vacuum* **84** 1029

[22] Wertheim G K, Riffe D M and Citrin P H 1994 *Phys. Rev.* B **49** 4834

[23] Hopman H J and Verhoeven J 1999 *Appl. Surf. Sci.* **150** 1

[24] Hopman H J, Zeijlemaker H and Verhoeven J 2001 *Appl. Surf. Sci.* **171** 197

[25] Whaley R and Thomas E W 1984 *J. Appl. Phys.* **56** 1505

[26] Sickafus E N 1977 *Phys. Rev.* B **16** 1436
Sickafus E N 1977 *Phys. Rev.* B **16** 1448

[27] Riccardi P, Sindona A, Barone P, Bonanno A, Oliva A and Baragiola R A 2003 *Nucl. Instrum. Methods Phys. Res.* B **212** 339

[28] Commisso M, Barone P, Bonanno A, Cimino R, Grosso D, Minniti M, Oliva A, Riccardi P and Xu F 2008 *J. Phys.: Conf. Ser.* **100** 092013